

# Reverse Engineering Point Clouds to Obtain Tensor Product B-Spline Surfaces by Blending Local Fits

Lavanya Sita Tekumalla  
*University of Utah*  
*lavanyat@cs.utah.edu*

Elaine Cohen  
*University of Utah*  
*cohen@cs.utah.edu*

May, 2005

## Abstract

*Being able to reverse engineer from point cloud data to obtain 3D models is important in modeling. As our main contribution, we present a new method to obtain a tensor product B-spline representation from point cloud data by fitting surfaces to appropriately segmented data. By blending multiple local fits our method is more efficient than existing techniques with the ability to deal with a detail by efficiently introducing a high number of knots. Further point cloud data obtained by digitizing 3D data, typically presents many associated complications like noise and missing data. As our second contribution, we propose an end-to-end framework for smoothing, hole filling, parameterization, knot selection and B-spline fitting that addresses these issues, works robustly with large irregularly shaped data containing holes and is straightforward to implement.*

## 1 Introduction

Digitizing 3D data and reverse engineering data to obtain 3D tensor product spline models has numerous applications in the field of CAD modeling and entertainment. Hence, the problem of automating design for manufacture and production by converting real world objects into computer models is extremely important. This paper focuses on processing noisy incomplete point clouds obtained from scanners and converting them to a tensor product spline representation with parameter values representative of the objects features.

3D data from real world objects obtained by scanning models is normally associated with several problems like noise in the data, missing data and holes. Incomplete data and holes in the data might typically lead to ill-behaved surfaces. Though surface in the hole regions is finally trimmed away after fitting, the area around holes might be affected and rank deficiencies might be encountered in the fitting phase. Further, most of the pa-

rameterization techniques do not deal with incomplete data.

**Contributions:** We propose a novel and efficient B-Spline surface fitting algorithm that blends local fits on segments of the data, with an automated knot placement strategy. We propose an end-to-end framework to reverse engineer point clouds with noisy data and holes in the data and fit tensor product B-spline surfaces that involves smoothing, hole filling, parameterization, knot selection and B-spline surface fitting steps.

We assume that an underlying triangular mesh structure is available with the data to obtain a good parameterization of the data. Where such information is not available, one could use existing meshing algorithms. We consider address models with an arbitrary number of holes, with the assumption that there is reasonable sampling density where triangulated data is available. We deal with a single patch of a segmented model that is homomorphic to a disc, with an arbitrary number of holes. Thus we do not aim to deal with issues such as approximating sharp features in the input and assume that such features do not exist in the input.

## 2 Prior Work

Though several aspects of the reverse engineering problem such as data parameterization, data fitting and knot selection have been extensively explored, there has not been significant work dealing with an entire pipeline for such a process for ill-conditioned input and data with holes in the input. B-spline surface fitting involves the steps of parameterization, knot placement and the actual fitting algorithm.

The task of parameterization involves finding a one to one mapping from every point on the surface to a point in a parametric domain. A lot of work has been done in this area to obtain planar maps for triangular meshes. A detailed discussion on these methods can be found in [10]. Once an initial mapping has been obtained, the pa-

parameterization can be improved using various criteria. In [13, 18, 3] iterative parameter correction is used to reparameterize the surface. In [19], the surface is reparameterized based on a stretch metric that measures the distortion in scale.

The traditional criterion for approximating data when there is more data than the degrees of freedom is the linear least squares method that minimizes the  $L^2$  norm of the residual. The weighted least squares technique is a related method that minimizes the least squares error and at the same time associates a weight with each error term based on its relative importance. One way of assigning weights while performing weighted least squares, is to define the weighting function with respect to a specific focus point. Therefore a different fit is obtained every time this point is changed. This method of weighting points is the basis for the MLS projection method described in section 2.1.

Several methods have attempted to address the additional problem of noise while fitting scattered data. One way to deal with scattered data is to minimize a combination of the  $L^2$  norm and the smoothing norm [11, 7].

Knot placement has a significant effect on the quality of the resulting surface during fitting. Several attempts [5, 16, 6] have been made to consider the least squares problem as a nonlinear optimization problem where the position of the knots is also optimized along with the control points. In [2], an iterative procedure is presented that inserts and deletes knots adaptively. However all these methods are computationally expensive and take significant execution time.

There exists some work on outlining an end-to-end framework for fitting B-spline surfaces to point clouds. In [11], a method to approximate scattered data that is triangulated using a single tensor product B-spline patch or hierarchical B-splines is presented. They minimize a functional that is a combination of the least squares distance and a fairing term based on data dependent thin plate energy in the fitting step. In [7], a framework is given for reverse engineering point clouds to get trimmed NURBS in which they too use a fairness term while minimizing error for fitting. However they parameterize data by projection and hence are not assured of finding a one to one mapping for all geometry.

Work has been done that attempts to deal with an entire model by making a network of B-spline patches. A method to construct B-spline models of arbitrary topology, by constructing a quadrilateral network of B-spline patches obtained by merging triangles in the input mesh appropriately is presented in [8]. In [14], another procedure is presented, where the user interactively segments the data. In [17], a method is described in which the model is segmented using K-means clustering and

then a NURBS patch network is computed. [12] decomposes the given point set into a quad-tree like data structure called a strip tree, to construct the patch network. Though some of these methods deal with the complex problem of handling the entire model, unlike this paper which deals with a single patch, none of these methods deal with holes and missing data. Further, our surface fitting technique of blending local fits to form a global fit is computationally efficient even with a large number of knots. Hence our method can be used to effectively deal with a higher level of surface detail, an important requirement in any realistic application.

## 2.1 Background : MLS Projection Procedure

In this section, we briefly review the MLS projection that is used through the various steps in our pipeline. The MLS projection procedure was proposed by [15] and [1] to deal with meshless surfaces. Given a point set, the MLS projection operator projects a point  $r$  near the surface onto the surface implicitly defined by the set of points. This surface can be defined as the set of points that project onto themselves.

The MLS projection operator proceeds in two steps. To project a point  $r$ , the first step requires finding an optimal local reference plane for the neighborhood of  $r$  by minimizing the  $L^2$  norm of the weighted perpendicular distance of points  $p_i$  in the neighborhood from the optimal reference plane. If  $n$  is the normal to the plane and  $t$  the distance of the plane from  $r$  (figure 1),  $\sum_{i=1}^N \langle n, p_i - r - tn \rangle^2 \theta(\|p_i - r - tn\|)$  is minimized with respect to  $n$  and  $t$ , where  $\theta$  is a gaussian weighting function defined as  $\theta(x) = e^{(-x^2/h)}$ . This is a non-linear minimization process. A local parameterization is obtained by projecting each point in the neighborhood onto this reference plane. The next step involves fitting a local bi-quadratic polynomial surface  $g$  using the moving least squares technique. That is, we find a  $g$  to minimize  $\sum_{i=1}^N (g(x_i, y_i) - f_i)^2 \theta(\|p_i - q\|)$  where  $q = r + tn$  ( $q$  is the projection on the best fit plane),  $(x_i, y_i)$  are the parameter values of  $p_i$  in the local reference plane and  $f_i = \langle p_i - q, n \rangle$  is orthogonal to the local reference plane. This polynomial when evaluated at the point  $q$ , gives the desired MLS projection.

We use the MLS projection procedure for smoothing and for filling holes in our framework.

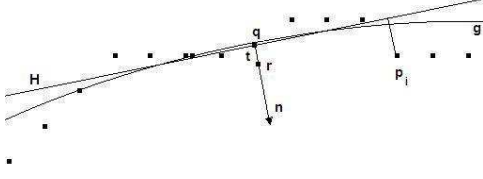


Figure 1: MLS Projection procedure for surfaces

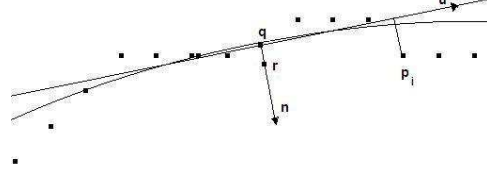


Figure 2: MLS Projection procedure for curves

### 3 Our Reverse Engineering Technique

We now present a framework that makes tensor product B-spline surfaces from triangulated point clouds. We propose a novel B-spline surface fitting algorithm based on blending local fits and an automated knot selection strategy in a later part of the section. We compare our fitting method with the traditional global least squares fit in terms of quality of fit and computation speed in the experiments section. Also, the effects of certain parameters of our method on the quality of the resulting fit, such as the choice of neighborhood size and the weighting function, are discussed.

In order to deal with noisy and incomplete data, we take a multi-stage approach of smoothing, hole filling, parameterization, knot selection and fitting. Each of these steps is detailed in the following sections.

#### 3.1 Smoothing

The smoothing step removes the noise and outliers in the data. Smoothing is achieved by projecting each point in the point cloud onto the MLS surface computed at that point. However, this method smooths the data in the local normal direction obtained through the MLS method. As a result, the boundary curve may contain significant noise even after smoothing the surface. That is, normals of the points in the boundary curve may not lie along the surface normals at these points. Hence, normal smoothing of the surface alone does not suffice.

We introduce an additional step of smoothing the boundary by projecting each point in the boundary onto the MLS curve computed locally at the point [20]. Suppose  $r$  is a noisy point near the curve, and  $q$  is its projection onto the line with direction vector  $u$ , we find the optimal line such that

$$\sum_{i=1}^N \|(p_i - q) - \langle p_i - q, u \rangle u\|^2 \theta(\|p_i - q\|)$$
 is minimized with respect to  $q$  and  $u$ . Again, this is a non-linear minimization process. The data is parameterized locally by projecting it onto the line along  $u$  and passing through  $q$ .

In the next step, the point  $p_i$  is projected onto a local quadratic approximation of the curve, in a process similar to [1]. First a local coordinate system is found, with  $u$ ,  $(r - q)$  and  $u \times (r - q)$  as the axes. Then the local neighborhood is transformed to this system. In order to handle 3D data, we treat the local curve as a parametric quadratic, and fit the curve  $(u, v(u), w(u))$  using the MLS approximation. Finally, the MLS projection is computed by evaluating the curve at  $u = 0$ .

Though we assume that the surface under consideration does not have any sharp corners, we cannot make the same assumption about the boundary. For instance a rectangular sheet that is segmented out has 4 sharp corners in the boundary though the interior is smooth. In order to preserve the sharp corners, the user is optionally permitted to specify the corners in the boundary so that each piece of the boundary is smoothed separately and the features preserved.

#### 3.2 Filling Holes

The MLS projection technique is used to fill holes in the input. Since a global parameterization of the data is not available, the filling procedure must be local to handle holes of arbitrary geometry. Hence we use the following method that is efficient and flexible [21].

1. For every pair of adjacent edges  $b_1$  and  $b_2$  in the boundary a new edge is introduced between the two edges, and hence a new triangle, if the angle between the  $b_1$  and  $b_2$  is less than  $\phi$ . Further, this edge is introduced only if it does not intersect any other boundary edge locally.

Since new boundary edges are introduced in this process, multiple passes of this step are made until no adjacent edges make an angle less than  $\phi$ .

2. For every edge  $e$  in the new boundary
  - (a) A local neighborhood of the mid-point of the edge and a local parameterization is found using the best fit plane using the MLS procedure.

- (b) A new point along the perpendicular bisector of  $e$  in the local parameterization is chosen, at a specified distance  $d(e)$ .
  - (c) A new point on the surface is computed using a local MLS approximation.
3. For every new point  $p$ , the closest edge in the current boundary is found. Let the end points of the edge be  $e_1$  and  $e_2$ . In order to ensure that well behaved triangles are obtained, a check is made to see if introducing a new triangle  $t$  with  $p$ ,  $e_1$  and  $e_2$  crosses any other boundary edge in the local parametric domain. If so, the point  $p$  is discarded. If not, a triangle  $t$  is introduced.
  4. If the boundary size is greater than 3, the entire process is repeated again starting from step 1. If not, a new triangle is introduced with the three vertices left in the boundary and the process ends.

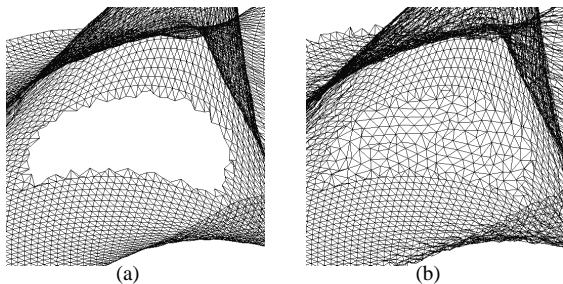


Figure 3: A close up view of the hole, filled using our method

The choice of  $d(e)$  and the value of  $\phi$  play a significant role in determining the shape of the triangulation. If  $\phi$  is too large, ill-shaped triangles result, that are elongated in one direction. We have obtained reasonable results for  $\phi$  of about  $5\pi/9$ . Some alternatives for choosing  $d(e)$  are to select a  $d(e)$  so that the resultant triangle is equilateral in the parametric domain with side  $e$ , where  $e$  is the side under consideration, or to create an isosceles triangle in the parametric domain with two of the sides as the average edge length  $a$ . We choose the later method and choose  $d(e)$  as  $\sqrt{(4a^2 - e^2)}/2$ .

### 3.3 Parameterization

We use mean value coordinates [9], to parameterize data. This method is a discretization of harmonic maps that are based on the fact that harmonic maps satisfy the mean value theorem. The method proceeds by mapping the boundary of the mesh to a convex polygon and solving a linear system of equations that express every

point as a convex weighted average of its neighbors in the parametric domain where the weights are obtained by the application of mean value theorem for harmonic functions.

An important issue that arises while using convex combination maps for parameterization is fixing the parameter values of the boundary to a convex polygon. When dealing with rectangle shaped objects, in order to obtain an intuitive parameterization, we let the user specify the boundary points that are fixed to the boundary of a rectangle. In other cases, we map the boundary of the object directly to a square by chord length.

### 3.4 Knot Placement

An important aspect of the fitting process is placing the adequate number of knots at the right locations. The knot placement strategy we use is to recursively subdivide the domain at the center of each region. The subdivision terminates when the data in the region can be fit locally with polynomial basis functions of degree 3, with an error no more than  $\kappa$ , where  $\kappa$  is measured as the average of the square root of sum of squares of errors of each point, or until a specific recursion depth is reached.

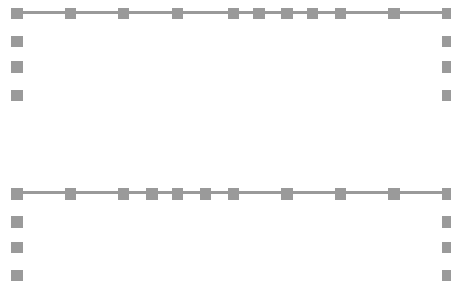


Figure 4: The knot vector obtained using hierarchical domain decomposition

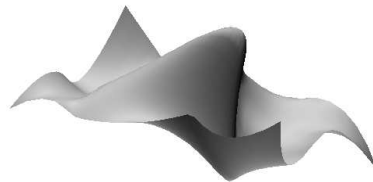


Figure 5: The surface under consideration

The knot vector finally contains the end points of all the patches along with additional knots added at the corners to make it open uniform. If there are  $n_p$  patches in the  $u$  direction, there are  $n_p + 1$  knots that are obtained from the end points of patches and hence there are  $n_p + 7$  knots in all when additional knots are added to make it

open cubic.

### 3.5 Fitting: Blending Local Fits

The fitting step produces a tensor product B-spline surface that represents the shape of the input, given the parameterization over a rectangular domain. We propose a new method based on blending local fits to obtain a global fit.

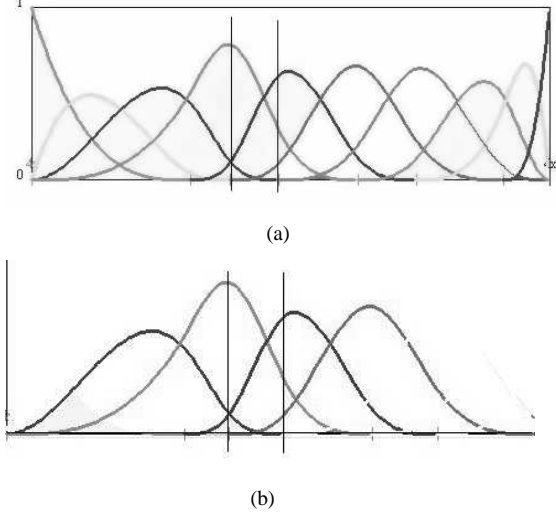


Figure 6: The first figure shows the global basis functions corresponding to the knot vector and the second figure shows the basis functions for a local fit in the particular interval

To illustrate our method, this section discusses the blending local fits method to fit B-spline curves. Suppose the hierarchical domain decomposition process leads to  $n_p$  patches, the knot vector has a size of  $n_p + 7$ , with  $n_p + 3$  basis functions. If the total number of data points is  $N$ , and we want to fit a B-spline curve

$\gamma = (t, f(t))$  where  $f(t) = \sum_{j=0}^{n_p+2} C_j \beta_{j,k}(t)$ , given data

points  $\{(t_i, f_i)\}_{i=0}^{N-1}$ , global least squares fit minimizes  $\sum_{i=0}^{N-1} (\sum_{j=0}^{n_p+2} C_j \beta_{j,k}(t_i) - f_i)^2$

Let the  $n_p$  segments resulting from the domain decomposition process be  $\{P_i\}_{i=0}^{n_p-1}$  and the mid-points of these patches be  $\{M_i\}_{i=0}^{n_p-1}$  and the number of points in each patch be  $\{N_i\}_{i=0}^{n_p-1}$ .

For each patch  $P_p$ , the coefficients of the local B-spline fit,  $L_0^p, L_1^p, L_2^p$  and  $L_3^p$  are found by applying the least squares criterion to the points in each patch by

minimizing  $\sum_{i \in N_i} (\sum_{j=0}^3 L_j^p \beta_{j+p,k}(t_i) - f_i)^2 w(t_i - M_p)$ .

where the function  $w$  is shown in figure 8.

In other words, the four basis functions used for any patch are the four B-spline basis functions that are non-zero in that patch as shown in figure 6.

The final curve is a blend of the local curve pieces that are fit independently, joined with  $C^2$  continuity. We attempt constructing a global control mesh where control points of each patch coincide with the appropriate control points of the neighbouring patches by the process of averaging control points of neighbouring patches as described below.

If  $\{G_i\}_{i=0}^{n_p+2}$  are the control points of the global mesh,  $G_i = r_0 L_3^{i-3} + r_1 L_2^{i-2} + r_2 L_1^{i-1} + r_3 L_0^i$  where  $(r_0 + r_1 + r_2 + r_3) = 1$ .

The first and the last terms of the above expression have less significance compared to the terms at the center because the control point  $G_i$  has lesser effect on patch  $P_{i-3}$  compared to  $G_{i-1}$  and  $G_{i-2}$ . Also, the weight given to points in the patch  $P_i$  is small while doing the local moving least squares fit for patch  $P_{i-1}$ , as discussed later. So we use the simplified weights of  $r_0 = r_3 = 0$  and  $r_1 = r_2 = 1/2$ .

Hence, in our scheme, the coefficients of the global control mesh are obtained as  $G_i = \frac{L_2^{i-2} + L_1^{i-1}}{2}$  for  $i$  from 2 to  $n_p + 2$ ,  $G_0 = L_0^0, G_1 = L_1^0, G_{n_p+1} = L_2^{n_p+1}$  and  $G_{n_p+2} = L_3^{n_p+2}$ . The coefficients of two adjacent segments are shown in the figure 7.

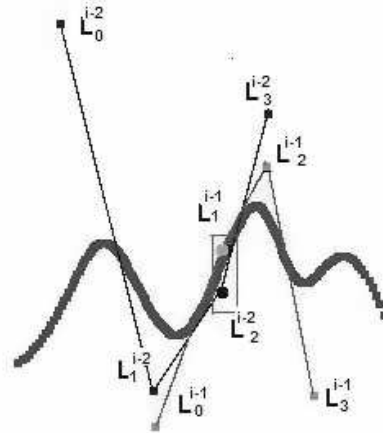


Figure 7: A figure showing the control polygons of two local patches and the process of blending

The local fit for a surface patch is done using local weighted least squares with respect to the mid-point of each patch in the parametric domain, in a way similar to the curve example. The basis functions used for the local fit are the tensor-product cubic B-spline basis functions that are non-zero in the interval under consideration.

Since 16 basis functions are non-zero for a given knot interval, upon performing the local fit, 16 coefficients are obtained. These are the 16 control points of a local patch. In order to obtain the control points that constitute the global control mesh, the control points of four adjoining patches corresponding to the same location in the parametric domain, are blended. At the boundaries, the control points of each pair of adjoining patches are blended.

To fit each individual patch, we consider points from the patch under consideration and the adjoining patches to get a smooth blend. Considering more points from other patches, while giving a smoother blend, might fail to capture some features in the input. We attempt to control this effect by using an appropriate weighting function.

The choice of weighting function used in this process affects the result significantly. We use a function that gives more weight to the interval under consideration and partial weight to the neighboring patches so that the local surface blends smoothly into the neighboring patches. With a knot vector  $\{t_0, t_1, \dots, t_i, t_{i+1}, \dots, t_n\}$ , we use the the windowing function in the curve case.

$$w(t) = \begin{cases} \frac{(t-t_i)^2}{e^{(t_i-t_{i-1})^2/4}} & t < t_i \\ 1 & t(i) \leq t \leq t_{i+1} \\ \frac{(t-t_{i+1})^2}{e^{(t_{i+1}-t_i)^2/4}} & t > t_{i+1} \end{cases}$$

Hence, we give full weight to the interval under consideration and decrease the weight exponentially beyond the interval as shown in figure 8. For surfaces, we construct two such windowing functions based on the knot vectors in the  $u$  and  $v$  directions and create a tensor product function.

This approach of taking a linear combination of control points to obtain the global mesh is not the optimal way of solving this problem and differs from the approach taken by the global least squares fit that tries to minimize the overall error of the fit rather than for each independent piece. A comparison of both methods is given in the next section.

### 3.5.1 Analysis of Blending Least Squares Fit

The preferred method for solving the linear least squares problem for data that is not well conditioned is the technique of singular value decomposition. This method takes a running time of the order  $4\ell m^2 - 4m^3 + O(\ell^2)$  where there are  $\ell$  data points and  $m$  control points to solve for. The blending local fits method provides substantial speed up computationally by using a constant  $m$  of 16 for each patch. Hence, if  $a$  is the number of rows and  $b$  the number of columns in the global control mesh, the blending local fits method solves  $(ab - 3a - 3b + 9)$

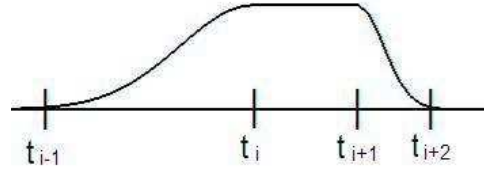


Figure 8: The weighting function that windows the neighborhood.

local systems and each local system has approximately  $9\ell/ab$  points. In effect the Blending local fits method reduces the runtime complexity of B-spline surface fitting from  $O(\ell m^2)$  to  $O(\ell)$ . Hence the size of the control mesh does not have much effect on the complexity of the fitting algorithm and considerable speedup can be realized for large control meshes.

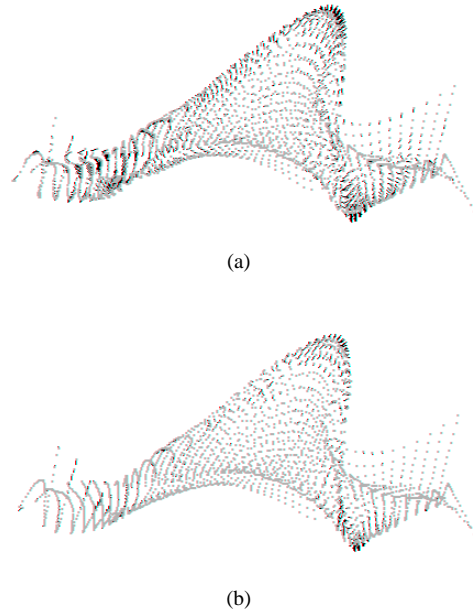


Figure 9: Lines indicating the distance between points on the fitted surface and the actual points for the same parameter value using the blending local fits method and the global least squares fit method.

The quality of fit obtained using the blending local fits method largely depends on size of the neighborhood chosen and the weighting function used. Figures

9(a) and 9(b) show the error obtained when approximating the data using the blending local fits method and the global least squares fit method respectively, with a  $13 \times 13$  control grid for 2500 points. We have taken a simpler version of our original input that we use later in order to perform the comparison in a reasonable amount of time, without the requirement of optimizing the fitting code to exploit the sparseness of the linear system. We obtain a fitting error of 0.098 per point while the global least squares fit achieves a 0.047 fitting error per point using the same knot vector. This is small compared to the feature size as shown in figure 9. Though a global least squares fit leads to a lower error than our fitting method, substantial computation time can be saved by using our fitting method.

## 4 Results

This section demonstrates the entire framework on the noisy data shown in figure 10 with 8100 points. Figure 11 shows the noise at the boundary is removed by smoothing the boundary as shown in figure 12. The hole in the input is then filled using the hole filling algorithm shown in section 3.2. The final fit, with a  $13 \times 13$  control mesh, as shown in figure 14 is obtained using the blending local fits method. The knot vector obtained using the adaptive domain decomposition technique is shown in figure 15.

## 5 Conclusion

This work outlines a framework to convert point cloud data with moderate complexity with associated triangulation information into tensor product B-spline surfaces or to fit a patch of the original segmented data set. This includes the multi-step approach of smoothing, hole filling, parameterization and finally fitting the surface. Though several patch-based methods and softwares already exist to solve the reverse engineering problem, this method aims to deal with point clouds that have problems like noise, holes in the geometry and missing data. Also this method aims to capture more detail in a single patch by deciding where to place the knots using a hierarchical subdivision of the domain and uses a combination of local weighted least squares approximations to find the control points of the tensor product surface as a whole.

## References

- [1] Marc Alexa, Johannes Behr, Daniel Cohen-Or, Shachar Fleishman, David Levin and Claudio T. Silva, "Computing and Rendering Point Set Surfaces", *IEEE Transactions on Computer Graphics and Visualization*, No.1 - 2003.

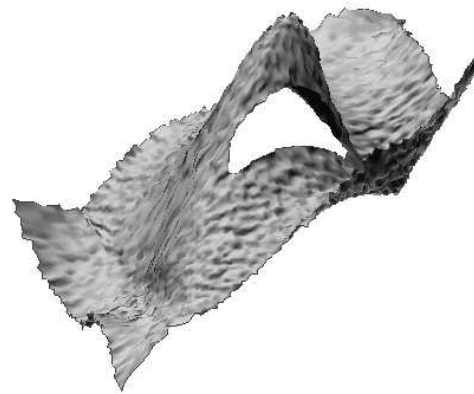


Figure 10: Noisy and incomplete data

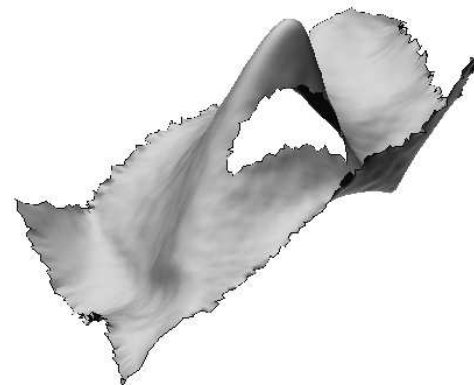


Figure 11: Smoothed data, without the boundaries smoothed

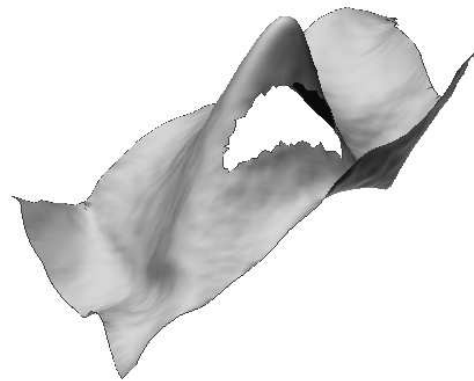


Figure 12: The smoothed surface

- [2] Baussard A.; Miller E.L.; Prmel D., "Adaptive B-spline scheme for solving an inverse scattering problem", *Inverse Problems*, 20 347-365, 2004.
- [3] Cohen, E. and O'Dell, C. L., "A Data Dependent Parametrization for Spline Approxima-

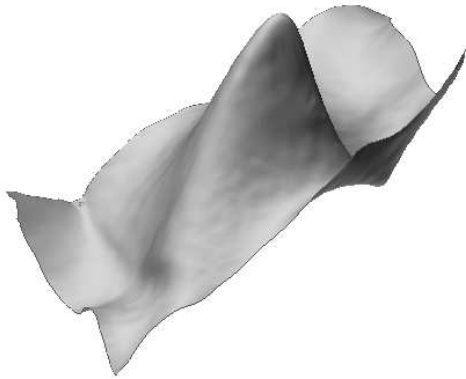


Figure 13: Hole filled

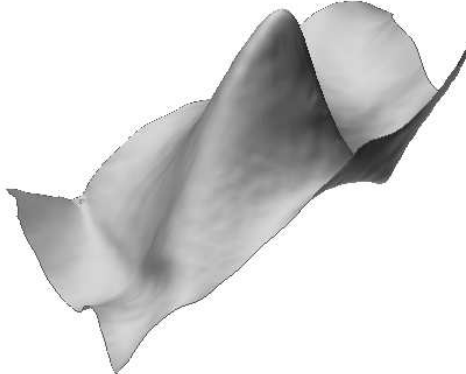


Figure 14: B-spline surface fit



Figure 15: Hole filled

tion", *Mathematical Methods in Computer Aided Geometric Design*, T. Lyche and L. L. Schumaker (eds.), 155166, 1989.

- [4] Elaine Cohen, Richard F Riesenfeld, Greshon Elber, *Geometric Modeling with Splines, An introduction*, A. K. Peters. Natick, Massachusetts, 2001.
- [5] De Boor, C. and Rice, J. R., "Least Squares Cubic Spline Approximation II- Variable Knots", *Tech Report, CSD TR 21, Purdue University*, April 1968.
- [6] Dierckx, P., "An Improved Algorithm for Curve Fitting with Parametric Functions", *Tech report TW54, Department of Computer Science, Katholieke University Leuven, Belgium*, 1981.

- [7] Dietz, U. and J. Hoschek, "Smooth B-spline Surface Approximation to Scattered Data", *Reverse Engineering*, J. Hoschek and W. Dankwort (eds.), B. G. Teubner, Stuttgart, 1996, 143-151
- [8] Matthias Eck, Hugues Hoppe, "Automatic reconstruction of B-spline surfaces of arbitrary topological type", *International Conference on Computer Graphics and Interactive Techniques archive Proceedings of the 23rd annual conference on Computer graphics and interactive techniques*, 1996.
- [9] Michael S. Floater, "Mean Value Coordinates", *Computer Aided Geometric Design*, 2003.
- [10] M. S. Floater and K. Hormann, *Advances on Multiresolution in Geometric Modelling*, N. Dodgson, M. S. Floater, and M. Sabin (eds.), Springer-Verlag, Heidelberg.
- [11] G. Greiner, K. Hormann, "Interpolating and Approximating Scattered 3D Data with Hierarchical Tensor Product Splines", *Surface Fitting and Multiresolution Methods*, A. Le Mhaut, C. Rabut, L.L. Schumaker (Eds.), 1996.
- [12] Benjamin F. Gregorski, Bernd Hamann, Kenneth I. Joy, "Reconstruction of B-spline Surfaces from Scattered Data Points", *Computer Graphics International*, pp. 163-172. 2000.
- [13] Josef Hoschek, Dieter Lasser, *The Fundamentals of Computer Aided Geometrical Design*, A K Peters, 1993.
- [14] Venkat Krishnamurthy, Marc Levoy, "Fitting Smooth Surfaces to Dense Polygon Meshes", *Proceedings of the 23rd annual conference on Computer graphics and interactive techniques*, p.313-324, August 1996.
- [15] Levin, D., "Mesh-independent surface interpolation", *Geometric Modeling for Scientific Visualization*, Edited by Brunnett, Hamann and Mueller, Springer-Verlag, 37-49, 2003.
- [16] David L. B. Jupp, "Approximation to Data by Splines with Free Knots", *SIAM Journal on Numerical Analysis*, Vol. 15, No. 2. (Apr., 1978), pp. 328-343.
- [17] I.K. Park, I.D. Yun, S.U. Lee, "Constructing NURBS Surface Model from Scattered and Unorganized Range Data", *Proc. 2nd International Conference on 3-D Digital Imaging and Modeling*, Ottawa, Canada, October 1999.
- [18] Michael Plass, Maureen Stone, "Curve-fitting with Piecewise Parametric Cubics", *ACM SIGGRAPH Computer Graphics*, *Proceedings of the 10th annual conference, on Computer Graphics and Interactive Techniques*, Volume 17, Issue 3, 1983.
- [19] P. V. Sander, S. J. Gortler, J. Snyder, H. Hoppe, "Signal-Specialized Parametrization", *Eurographics Workshop on Rendering*, 2002.
- [20] Lavanya S. Tekumalla, Elaine Cohen, "Smoothing Space Curves with the MLS Projection" *Proceedings of Geometric Modeling, Visualization and Graphics*, July 2005.

- [21] Lavanya S. Tekumalla, Elaine Cohen, "A Hole Filling Algorithm for Triangle Meshes", *Technical Report, School of Computing, University of Utah, UUCS-04-019*.
- [22] Jianning Wang and Manuel M. Oliveira. "A Hole Filling Strategy for Reconstruction of Smooth Surfaces in Range Images", *XVI Brazilian Symposium on Computer Graphics and Image Processing*. So Carlos, SP. October 12-15, 2003.